Supporting Information

Species Dependent Metabolism of a Covalent nsP2 Protease Inhibitor with *in Vivo* Anti-alphaviral Activity.

Mohammad Anwar Hossain[†,#], Abigail K. Mayo[‡], Anirban Ghoshal[†,#], Sharon A. Taft-Benz[§,#], Elizabeth J. Anderson[§,#], Noah L. Morales[§,#], Katia D. Pressey[§,#], Ava M. Vargason[▽,#], Kim L. R. Brouwer[‡], Nathaniel J. Moorman[§,#], Mark T. Heise[⊥,§,#], and Timothy M. Willson[†,#,*]

[†]Structural Genomics Consortium, UNC Eshelman School of Pharmacy, University of North Carolina at Chapel Hill, Chapel Hill, NC 27599, USA.

[#]READDI AViDD Center, University of North Carolina at Chapel Hill, Chapel Hill, NC 27599, USA.

[‡]Division of Pharmacotherapy and Experimental Therapeutics, UNC Eshelman School of Pharmacy, University of North Carolina at Chapel Hill, Chapel Hill, NC 27599, USA

[§]Department of Microbiology and Immunology, University of North Carolina at Chapel Hill, Chapel Hill, NC, 27599, USA

[▽]Eshelman Innovation, UNC Eshelman School of Pharmacy, University of North Carolina at Chapel Hill, Chapel Hill, NC 27599, USA

[⊥]Department of Genetics, University of North Carolina at Chapel Hill, Chapel Hill, NC, 27599, USA

*Correspondence: tim.willson@unc.edu

Table of Contents

Table S1. Plasma Protein Binding of 1[a]

Species	Protein binding (%)	f_u
Mouse	82	0.18
Rat	89	0.11
Dog	80	0.20
Human	86	0.14

[a] Plasma protein binding was determined by equilibrium dialysis. For monkey, the human value used.

Table S2. Equations for Allometric Scaling

Calculated Value	Equation
Systemic Clearance	$CL_s = \frac{F \times X_0}{AUC_{PO}}, where\ F = \frac{AUC_{PO}}{AUC_{IV}} \times \frac{X_{0,IV}}{X_{0,PO}}$
Intrinsic Clearance[a]	$CL_{int,in\ vivo} = \frac{hepatocellularity\ (\frac{10^6 cells}{g\ liver}) \times \frac{liver\ weight\ (g)}{kg\ body\ weight\ (kg)} \times CL_{int,in\ vitro}(\mu L/min/10^6 cells)}{fu_{in\ vitro}}$
IVIVE Scaling Factor[b]	$Scaling\ factor = hepatocellularity\ (10^6 cells/g\ liver) \times liver\ weight\ (g/kg) \times \frac{1\ mL}{1000\ uL}$
Blood Clearance	$CL_{int,blood} = CL_{int,plasma} \times \frac{C_{plasma}}{C_{blood}}$
Hepatic Clearance	$CL_h = \frac{Q_{blood} \times fu \times CL_{int,in\ vivo}}{Q_{blood} + fu \times CL_{int,in\ vivo}}$
Hepatic Extraction	$E_{hepatic} = \frac{\frac{Q_{blood} \times fu \times CL_{int,in\ vivo}}{Q_{blood} + fu \times CL_{int,in\ vivo}}}{Q_{blood}} = \frac{CL_h}{Q_{blood}}$
i.v. Infusion Rate	$k_0 = infusion\ rate = C_{ss} \times CL$

[a]Calculations assumed $fu_{in\ vitro} = 1$

[b]Values from Petersson, C., Zhou, X., Berghausen, J., Cebrian, D., Davies, M., DeMent, K., & Baker, J. (2022). Current approaches for predicting human PK for small molecule development candidates: findings from the IQ human PK prediction working group survey. The AAPS journal, 24(5), 85. https://doi.org/10.1208/s12248-022-00735-9

Table S3. Blood to Plasma Ratios of 1

	Blood:plasma ratio ($K_{b/p}$)[a]
Rat	1.37
Monkey	1.41
Human	1.12

[a]For Mouse and Dog a nominal value of 1.0 was used in IVIVE calculations based on measured values in the other species.

Figure S1. MS fragmentation of metabolites M1–18 from mouse plasma

M1

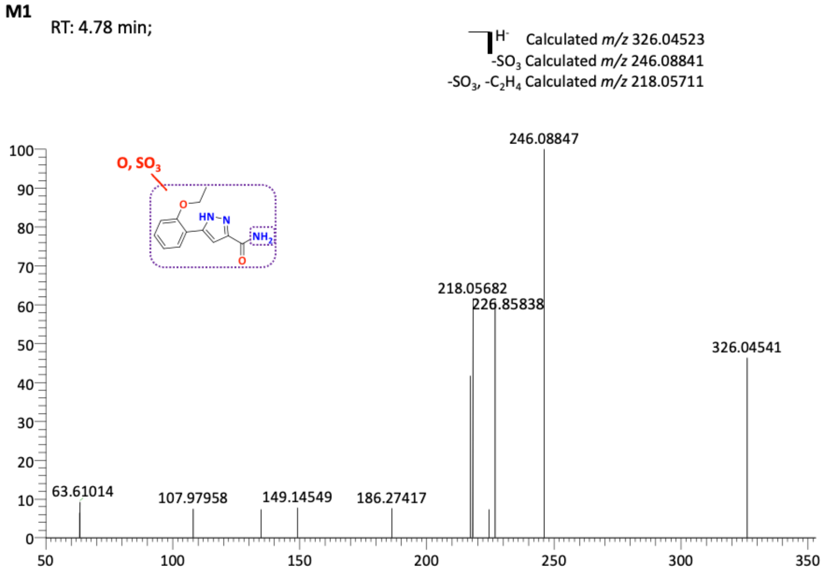

M2

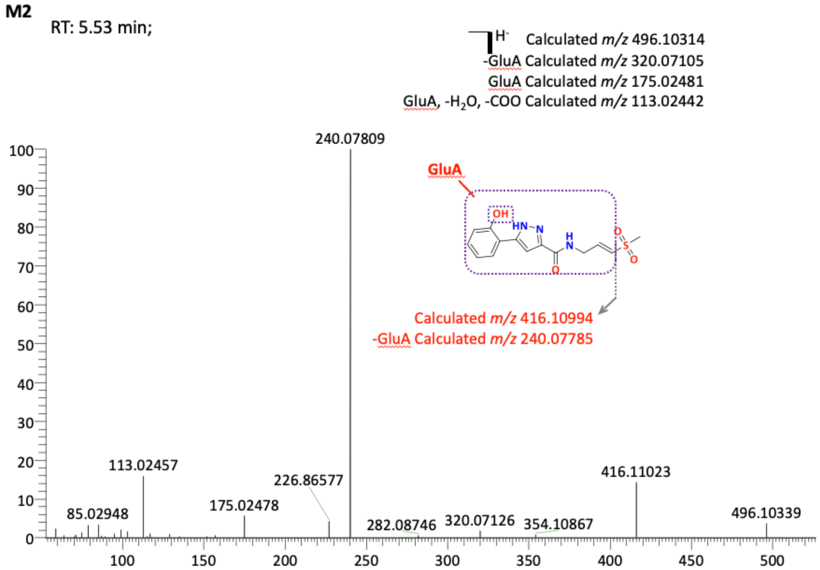

M3

RT: 5.60 min;

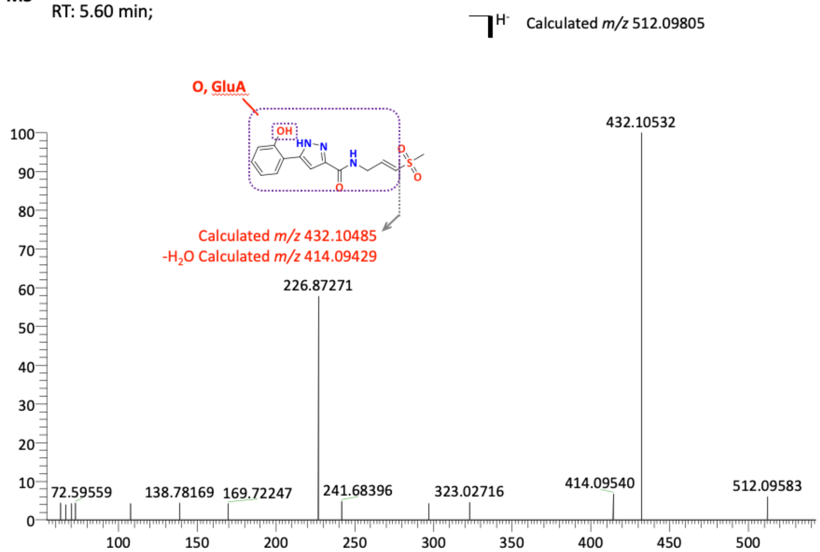

M4

RT: 5.62 min;

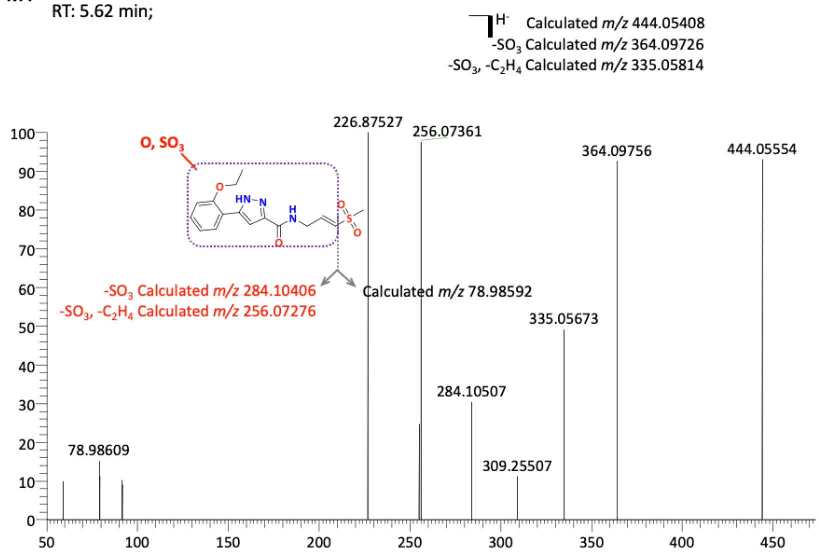

M5

RT: 5.72 min;

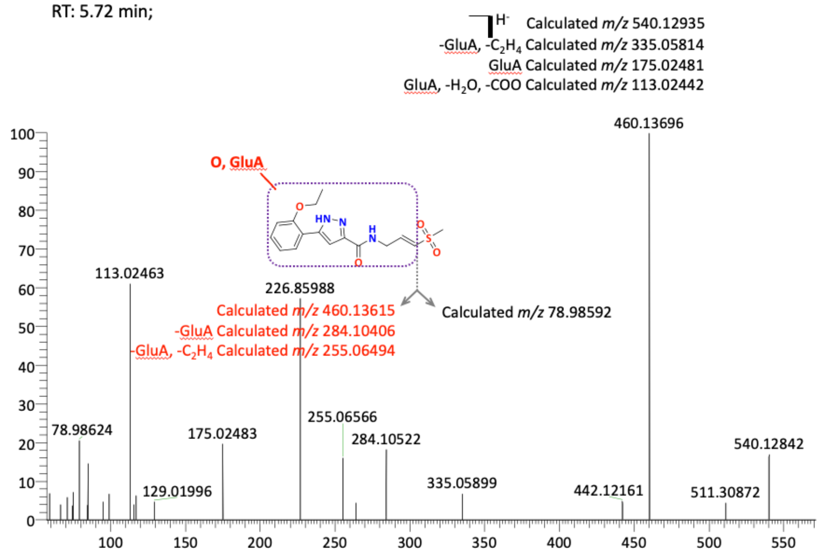

M6

RT: 6.06 min;

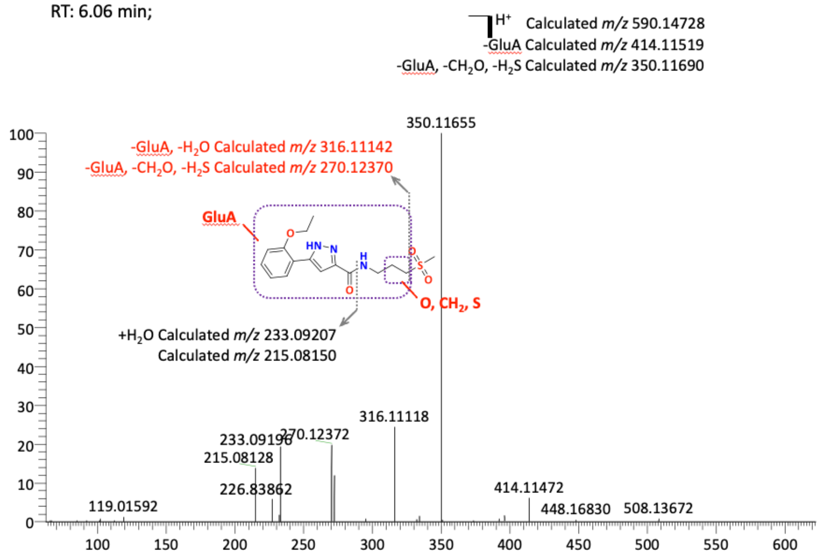

M7

RT: 6.16 min;

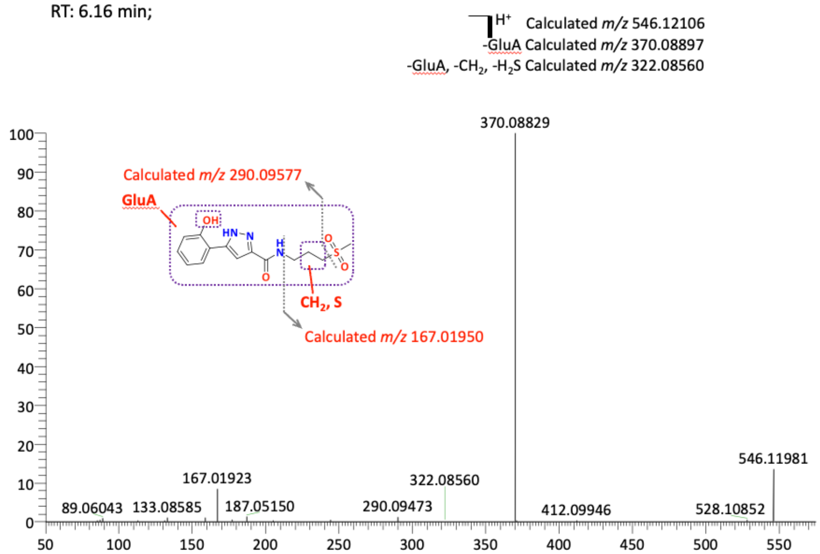

M8

RT: 6.29 min;

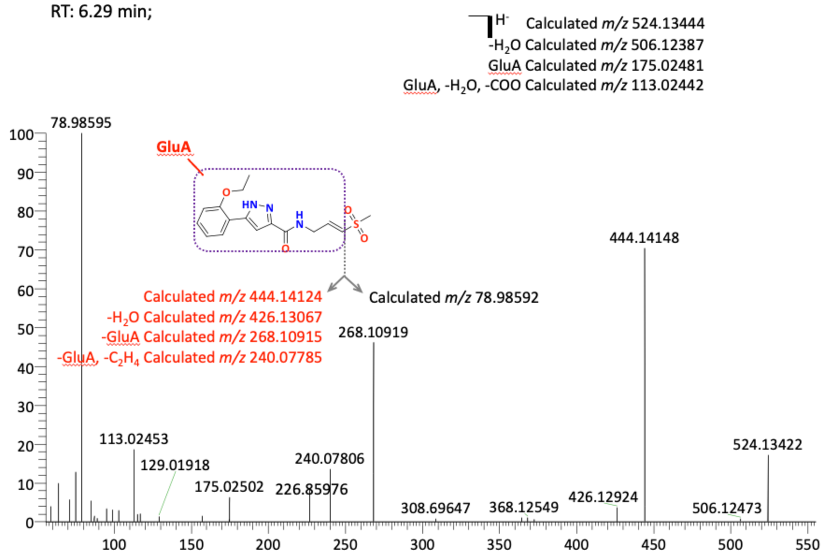

M9

RT: 6.50 min;

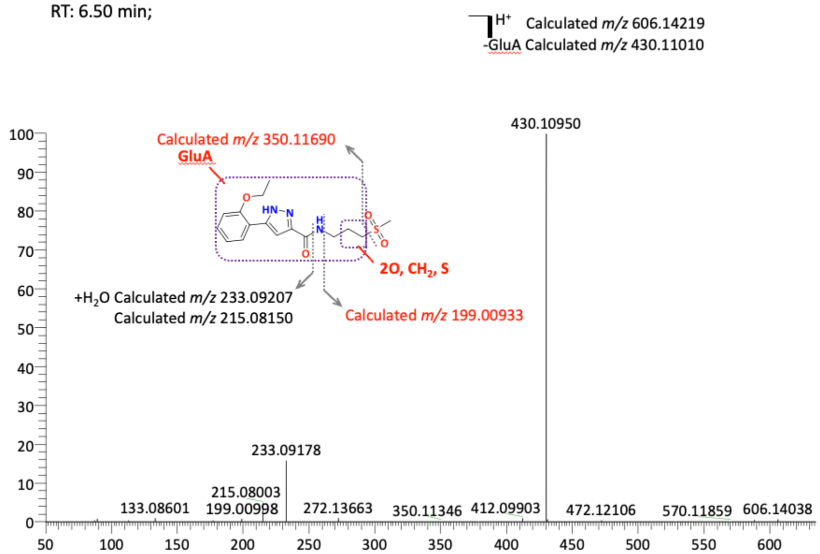

M10

RT: 6.70 min;

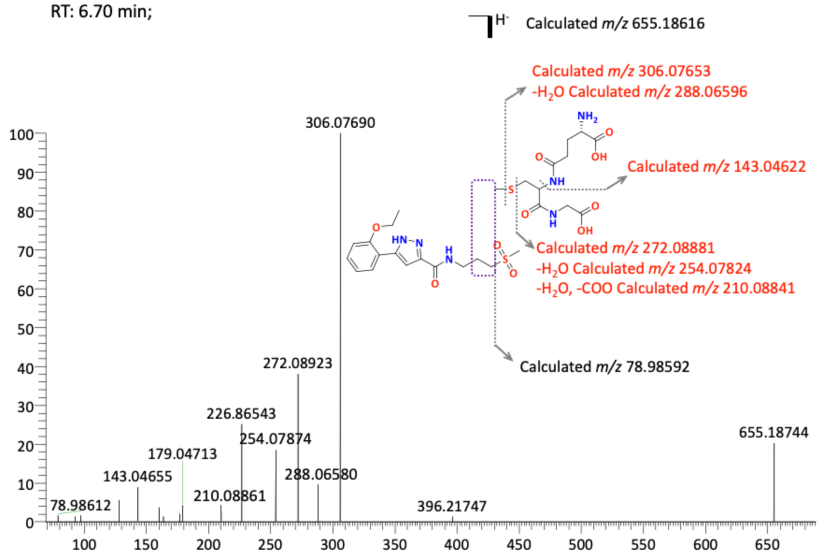

M11

RT: 6.74 min;

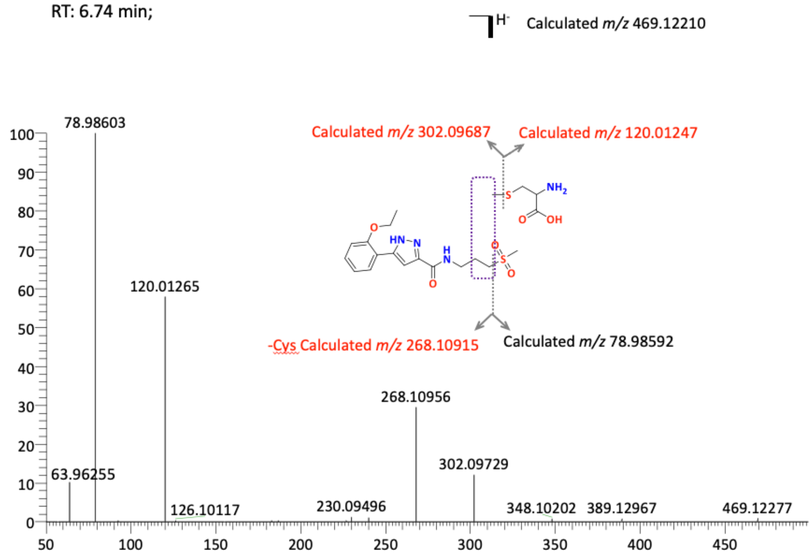

M12

RT: 6.81 min;

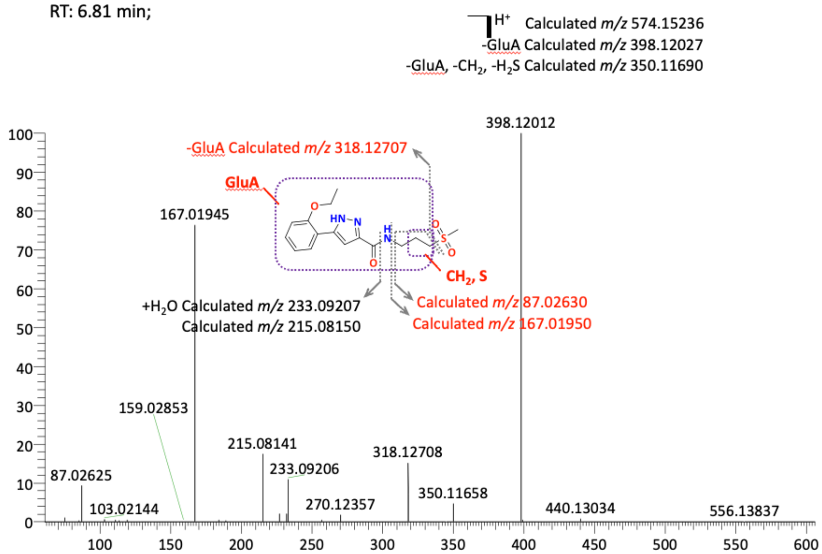

M13

RT: 7.02 min;

$]H^-$ Calculated *m/z* 460.13615
-GluA Calculated *m/z* 284.10406

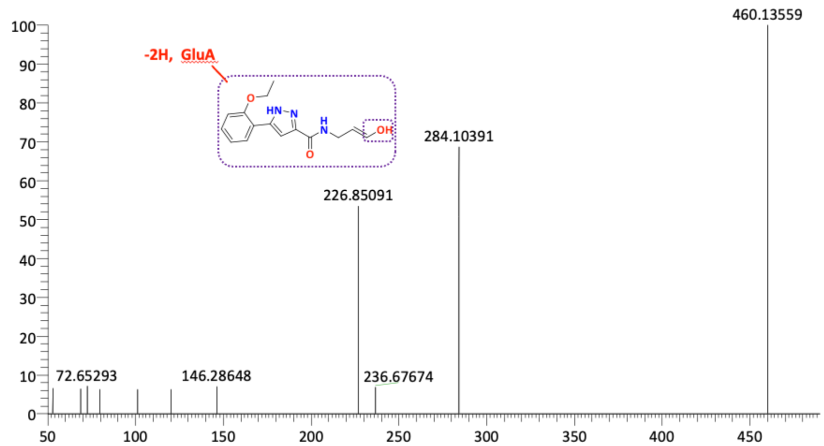

M14

RT: 7.49 min;

$]H^+$ Calculated *m/z* 232.10805
$-NH_3$, $+H_2O$ Calculated *m/z* 233.09207
$-NH_3$ Calculated *m/z* 215.08150

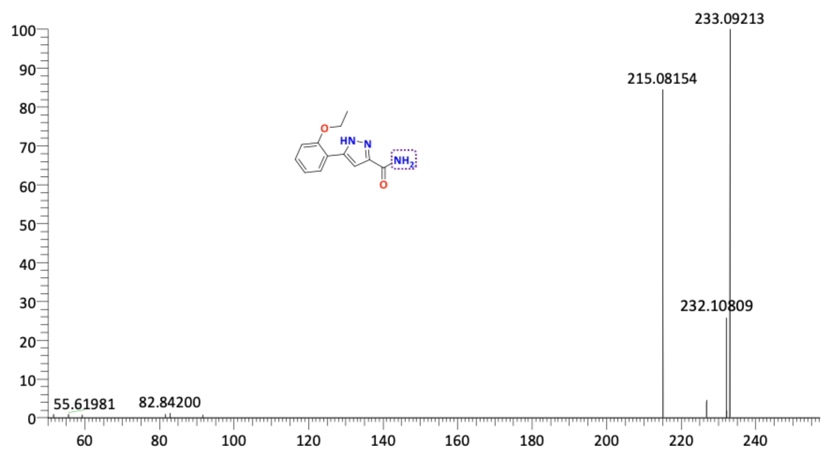

M15

RT: 7.75 min;

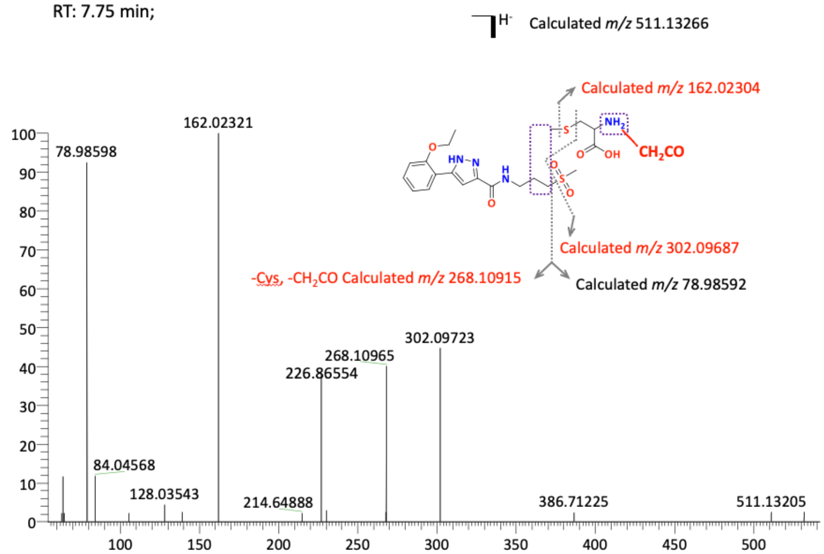

M16

RT: 8.06 min;

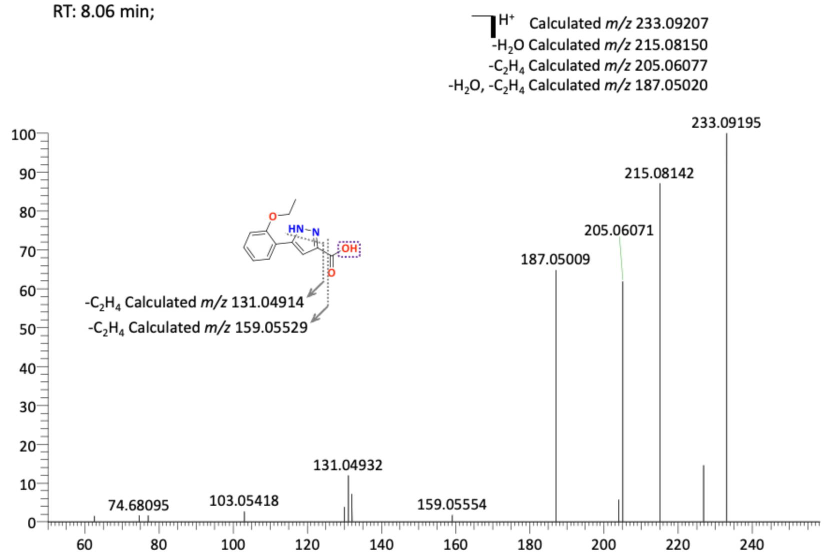

M17

RT: 8.34 min;

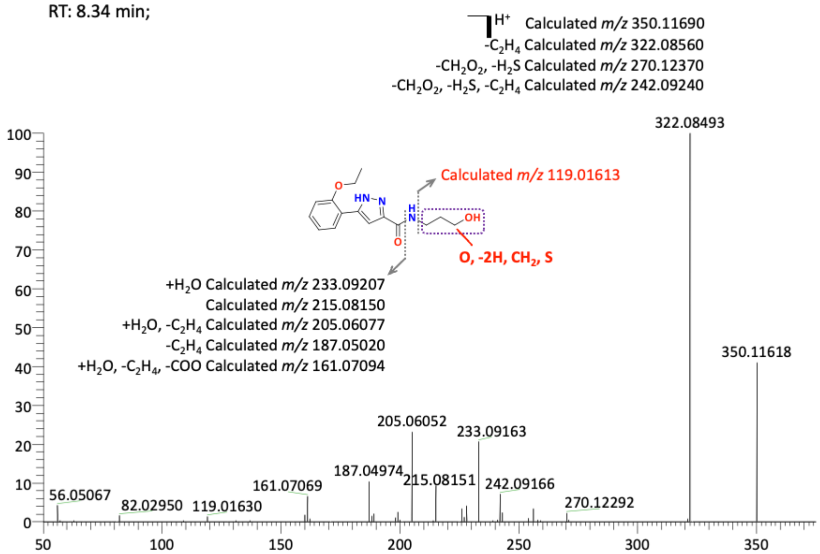

M18

RT: 8.97 min;

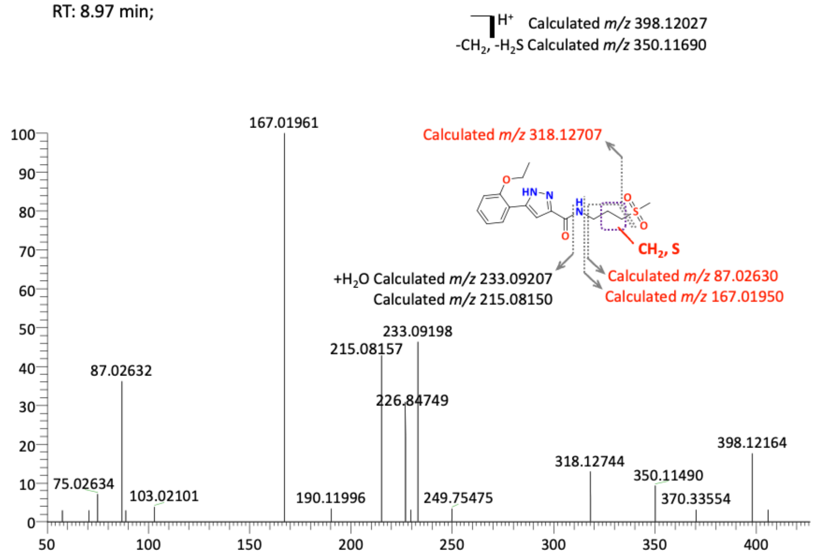

Figure S2. MS fragmentation of metabolites M1–22 from hepatocytes

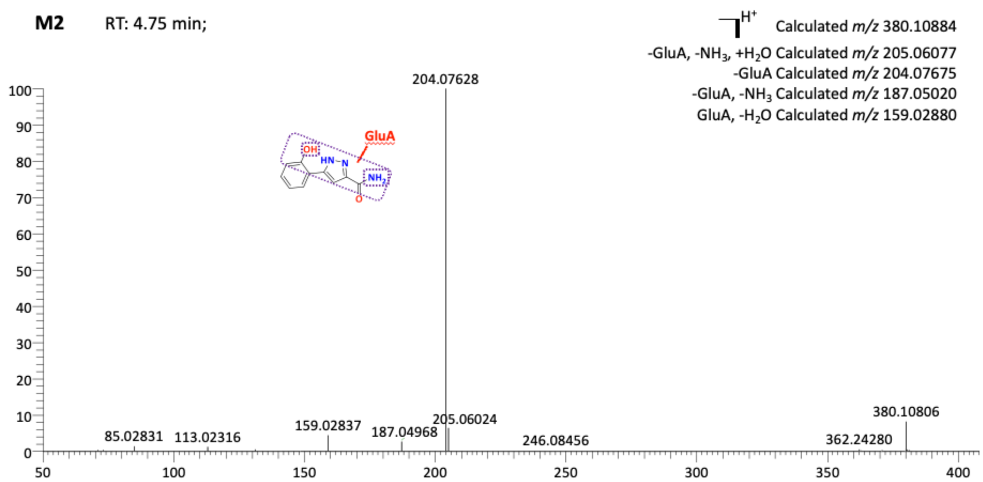

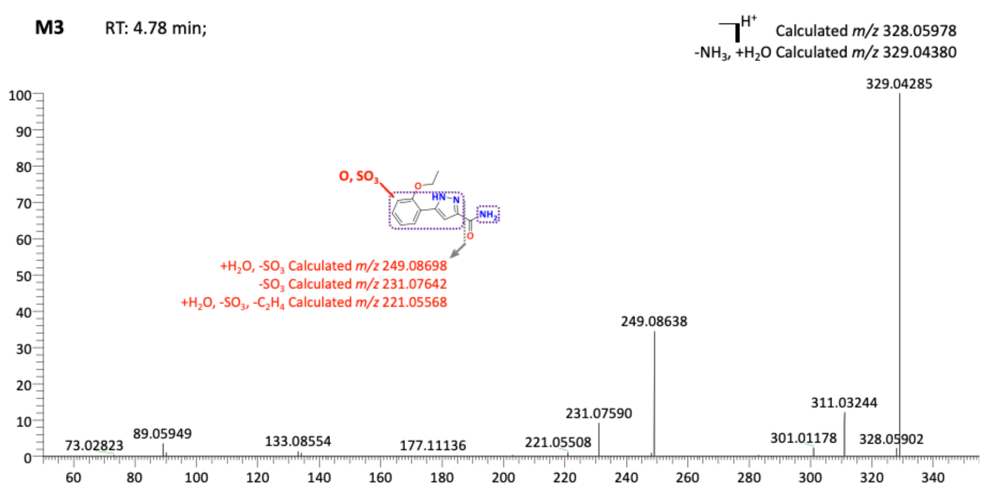

M4 RT: 5.54 min;

$]^{H^+}$ Calculated *m/z* 498.11769
-GluA Calculated *m/z* 322.08560

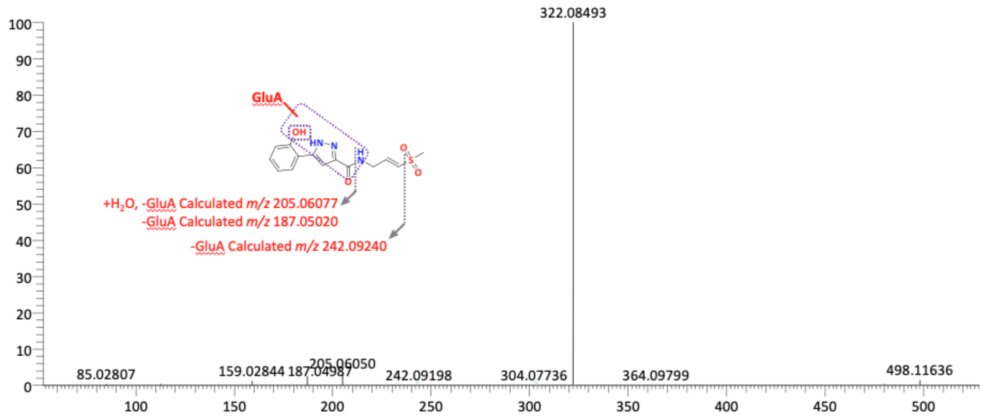

M5 RT: 5.60 min;

$]^{H^+}$ Calculated *m/z* 498.11769
-GluA Calculated *m/z* 322.08560

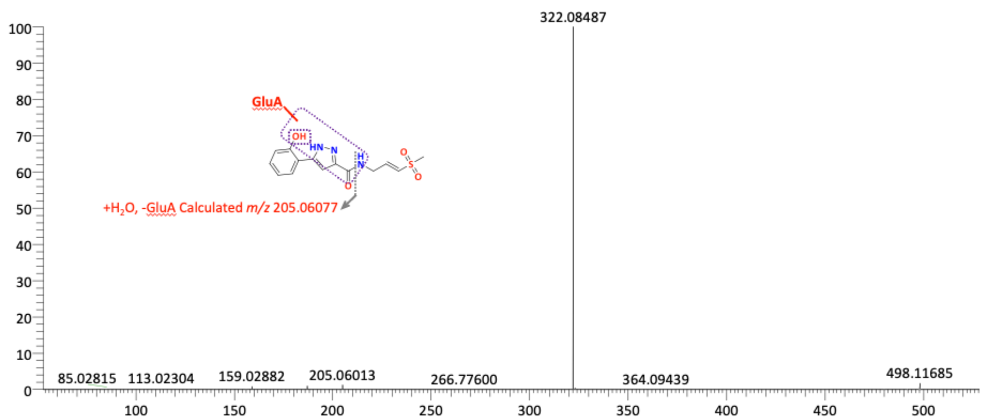

M6 RT: 5.61 min;

$]^{H^+}$ Calculated *m/z* 629.16941
-H_2O Calculated *m/z* 611.15885

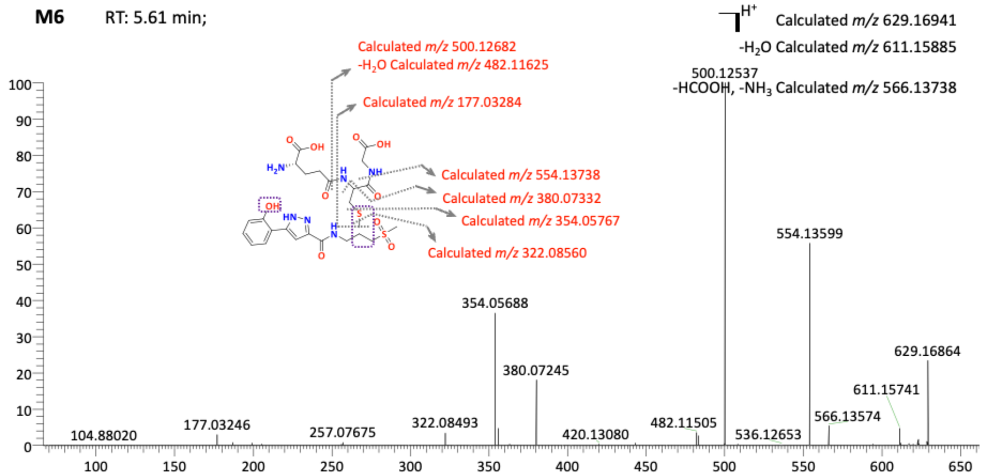

M7 RT: 5.76 min;

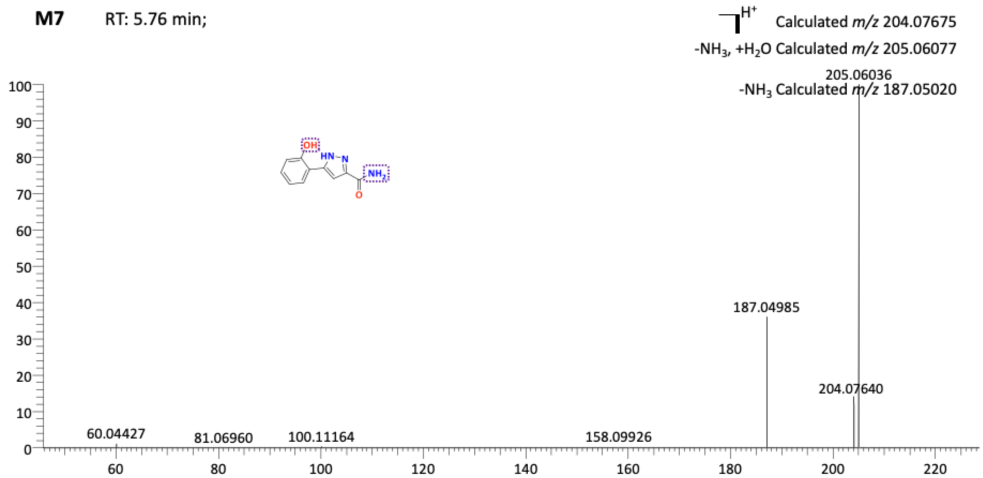

M8 RT: 6.73 min;

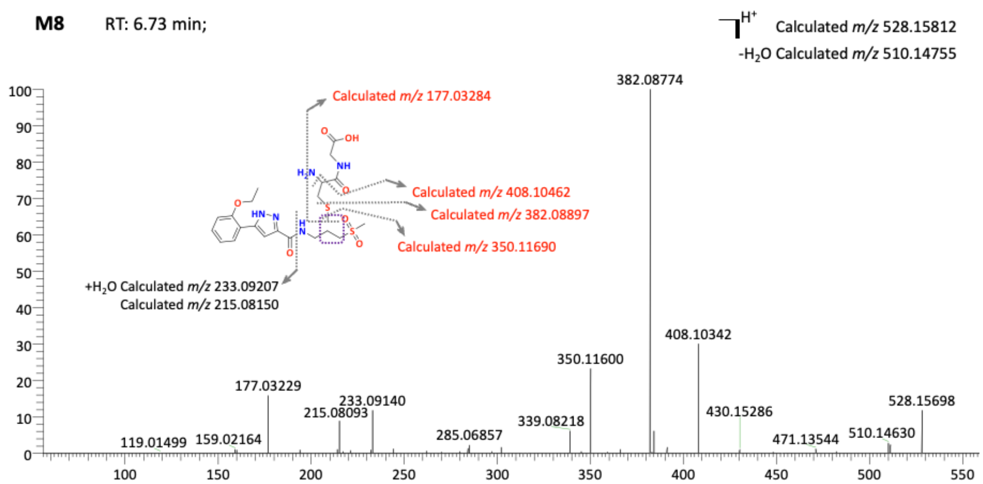

M9 RT: 6.74 min;

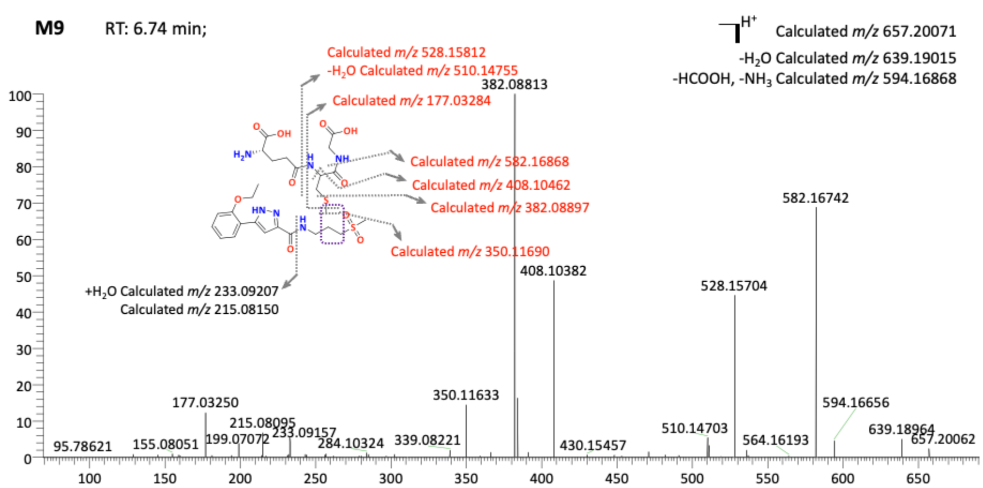

M10 RT: 6.76 min;

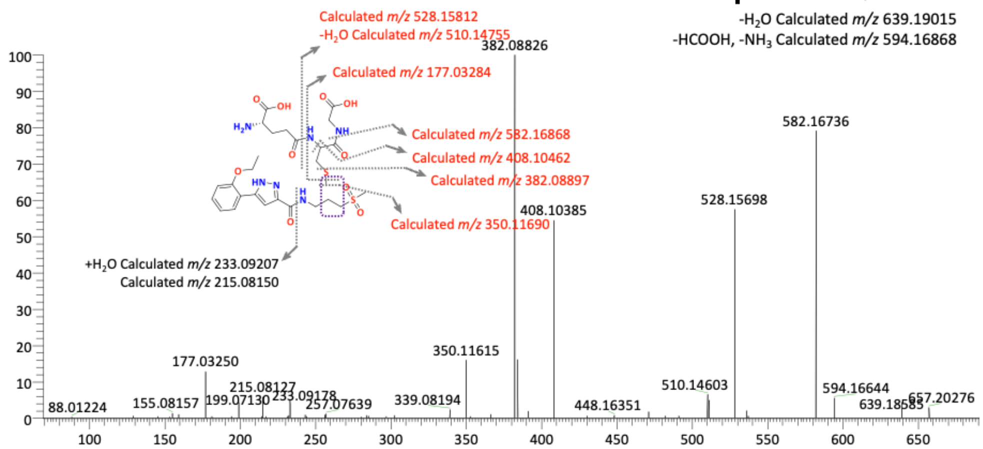

M11 RT: 6.79 min;

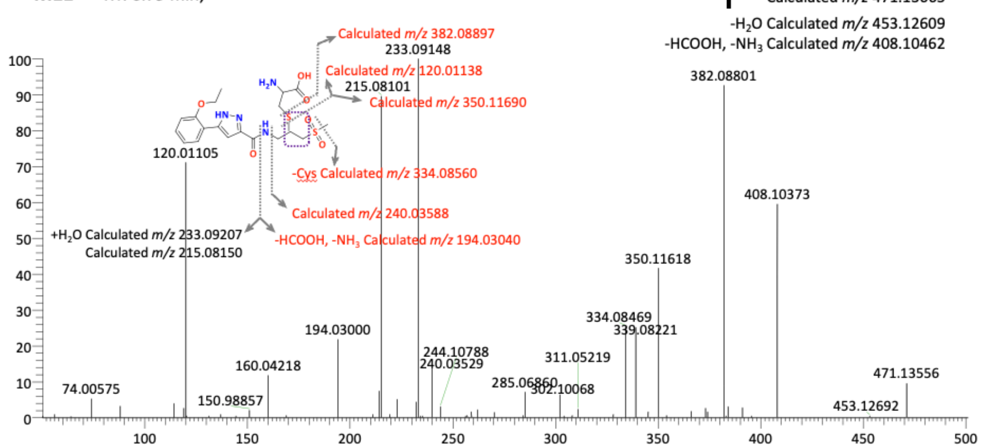

M12 RT: 6.97 min;

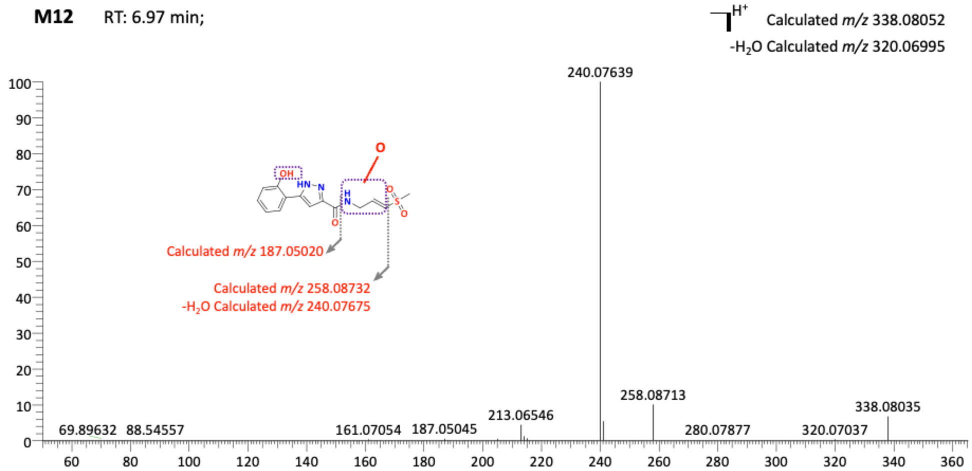

M13 RT: 7.15 min;

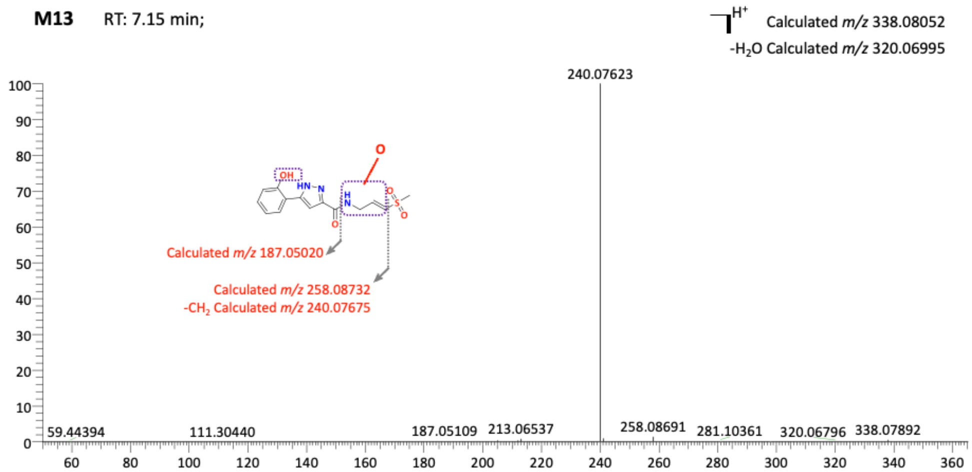

M14 RT: 7.25 min;

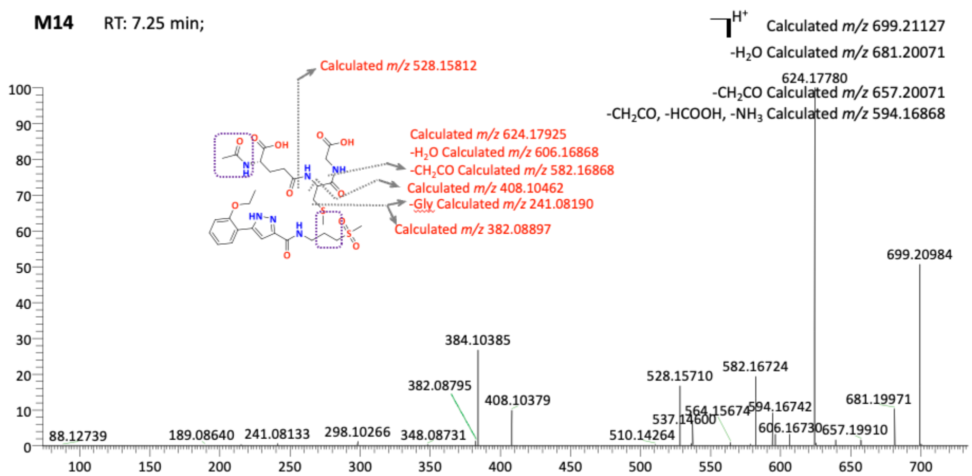

M15 RT: 7.33 min;

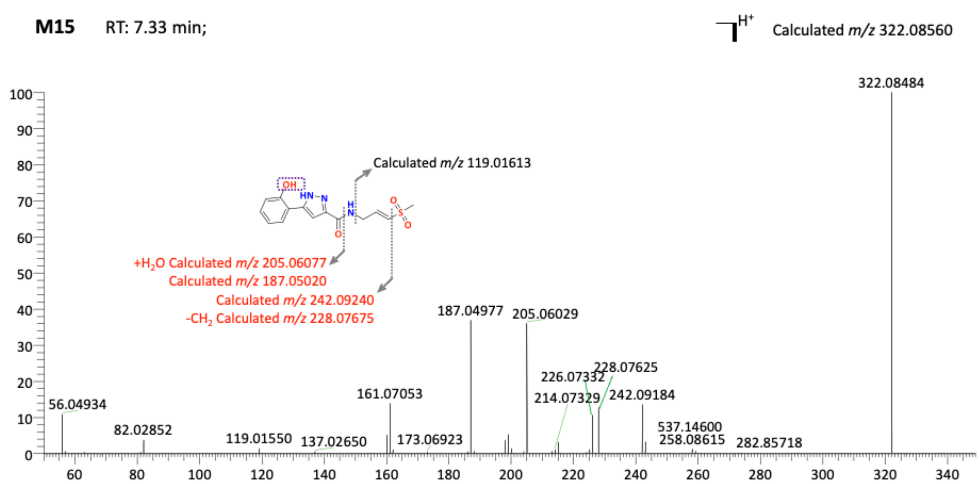

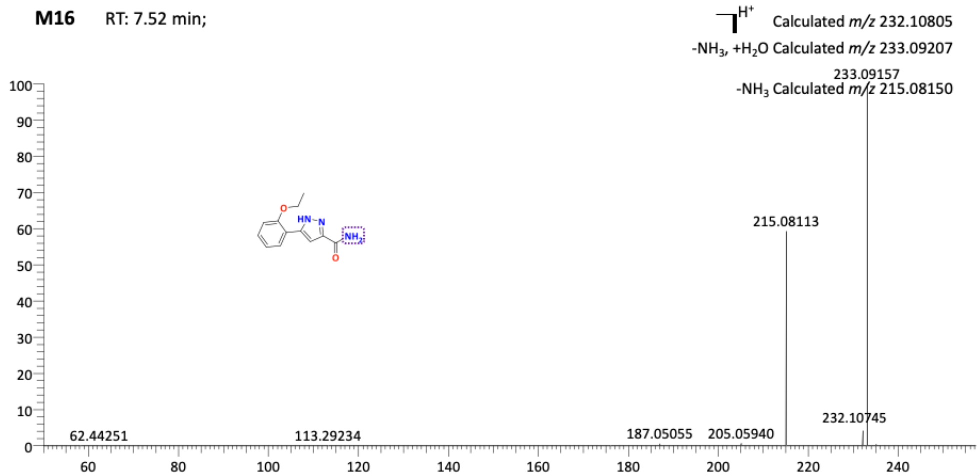

M16
RT: 7.52 min;
Calculated m/z 232.10805
-NH3, +H2O Calculated m/z 233.09207
-NH3 Calculated m/z 215.08150
233.09157
215.08113
232.10745
62.44251
113.29234
187.05055
205.05940

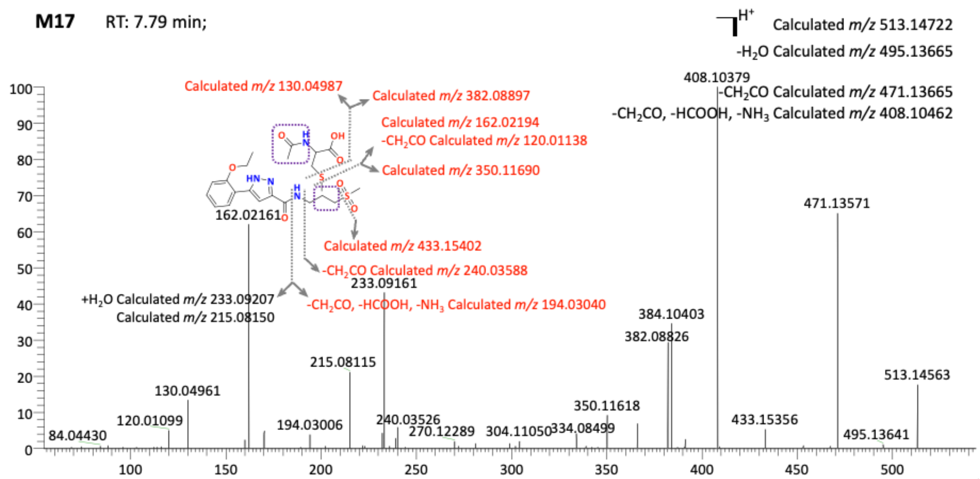

M17
RT: 7.79 min;
Calculated m/z 513.14722
-H2O Calculated m/z 495.13665
-CH2CO Calculated m/z 471.13665
-CH2CO, -HCOOH, -NH3 Calculated m/z 408.10462
Calculated m/z 130.04987
Calculated m/z 382.08897
Calculated m/z 162.02194
-CH2CO Calculated m/z 120.01138
Calculated m/z 350.11690
Calculated m/z 433.15402
-CH2CO Calculated m/z 240.03588
-CH2CO, -HCOOH, -NH3 Calculated m/z 194.03040
+H2O Calculated m/z 233.09207
Calculated m/z 215.08150
408.10379
471.13571
162.02161
233.09161
384.10403
382.08826
215.08115
513.14563
130.04961
350.11618
120.01099
433.15356
194.03006
240.03526
270.12289
304.11050
334.08499
495.13641
84.04430

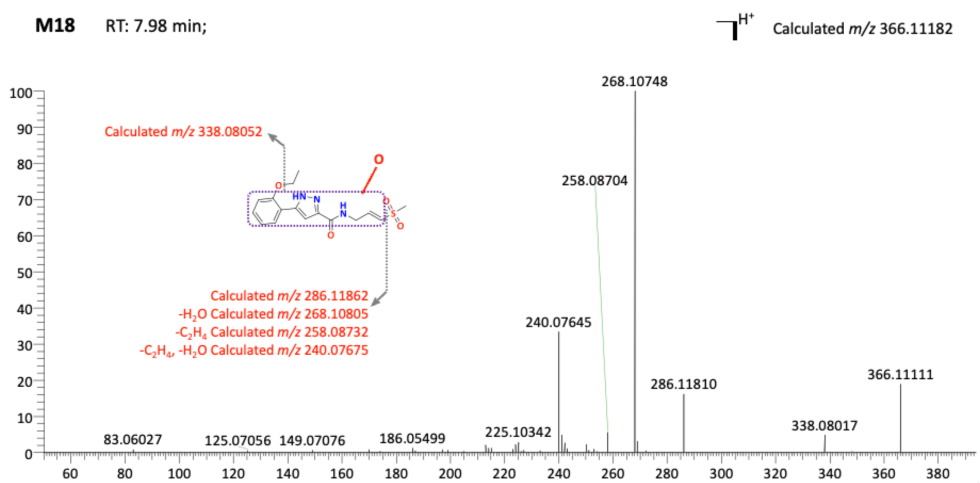

M18
RT: 7.98 min;
Calculated m/z 366.11182
Calculated m/z 338.08052
Calculated m/z 286.11862
-H2O Calculated m/z 268.10805
-C2H4 Calculated m/z 258.08732
-C2H4, -H2O Calculated m/z 240.07675
268.10748
258.08704
240.07645
286.11810
366.11111
338.08017
83.06027
125.07056
149.07076
186.05499
225.10342

M19 RT: 8.03 min;

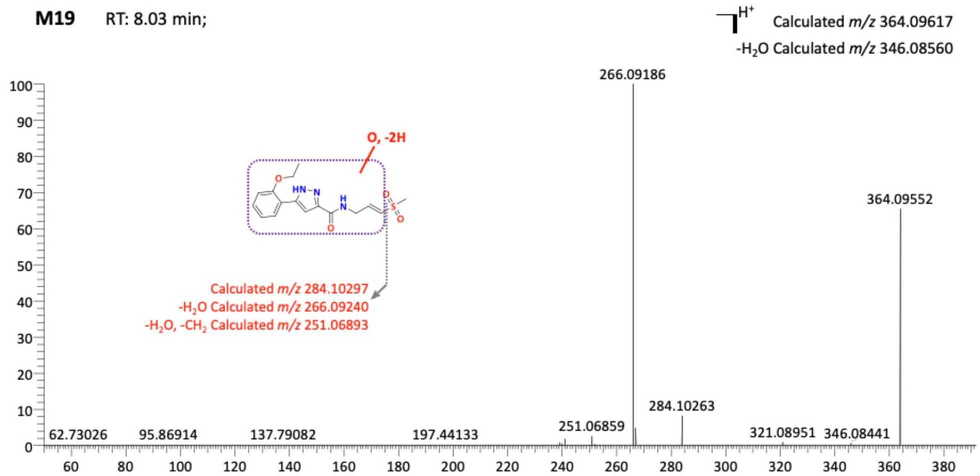

M20 RT: 8.08 min;

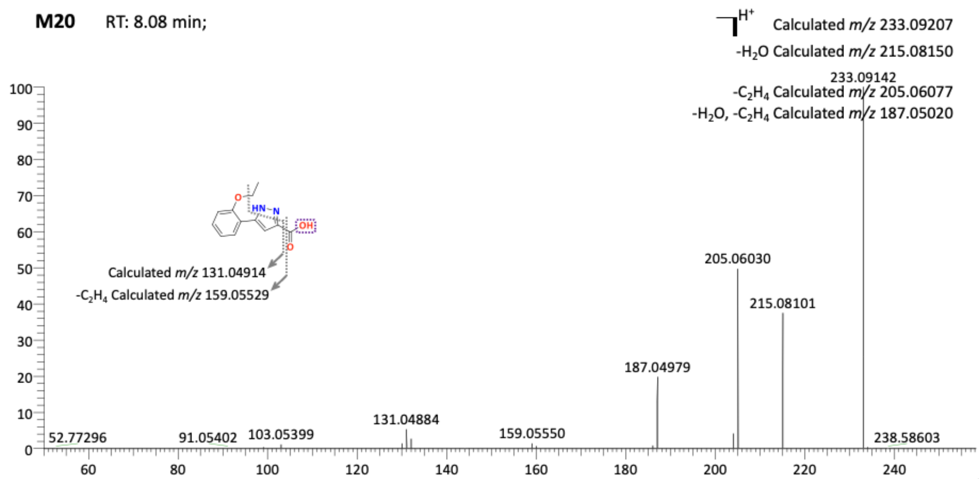

M21 RT: 8.39 min;

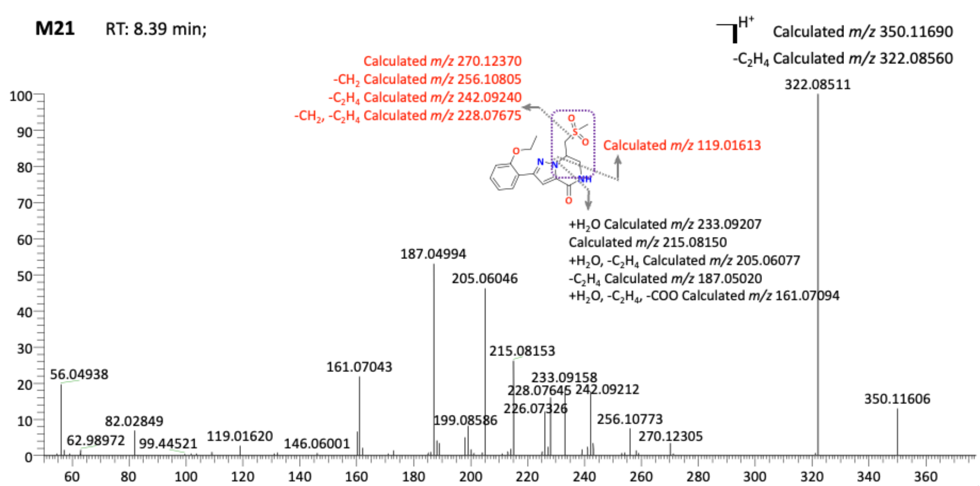

M22 RT: 8.50 min;